

Fig. 1. 3D rendering of PANDA facility [19].

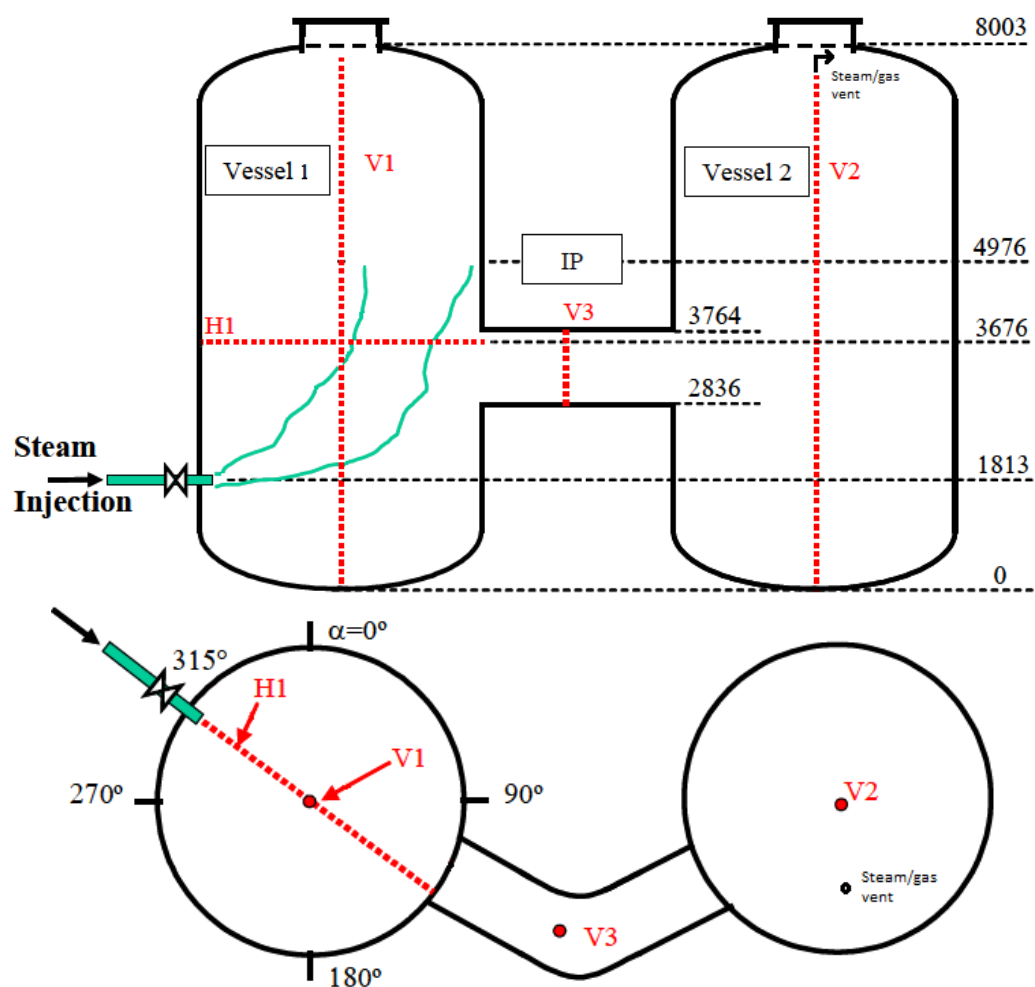
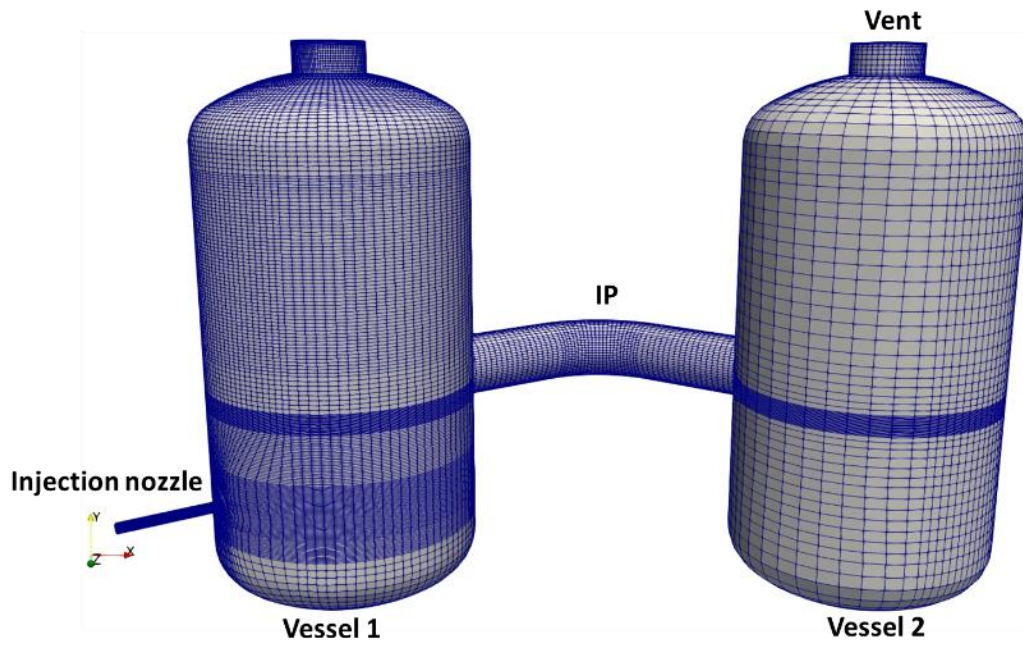
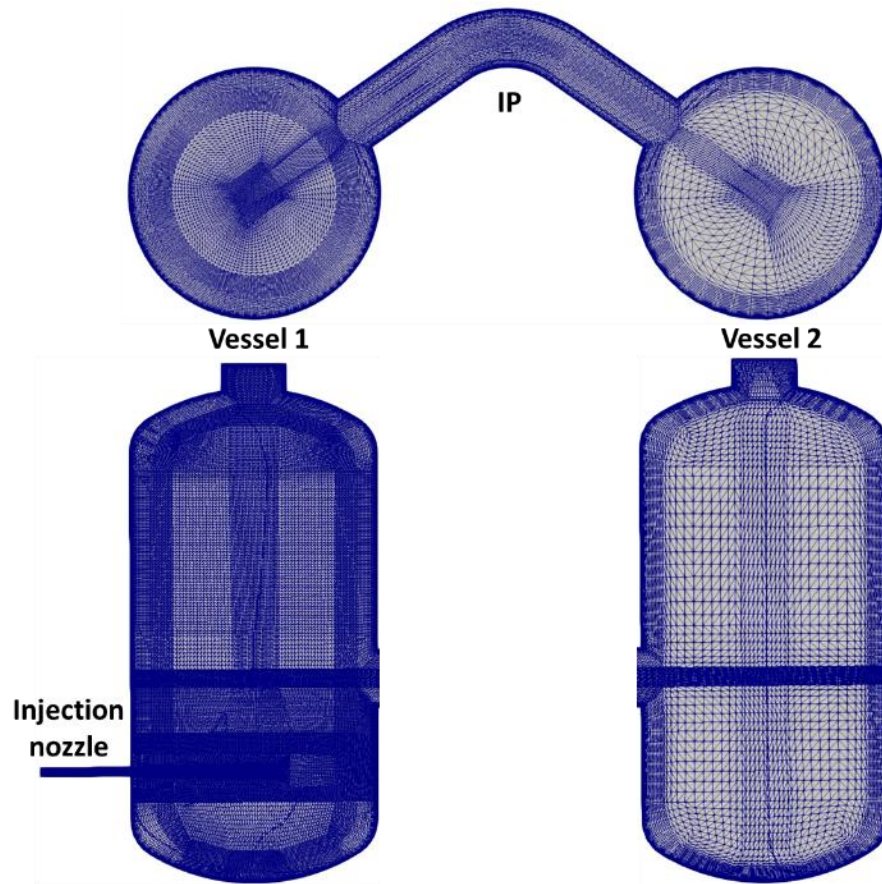


Fig. 2. Configuration of SETH Test 16 [10].



(a) Front view



(b) Cross section

Fig. 3. Schematic of the computational domain with mesh grid.

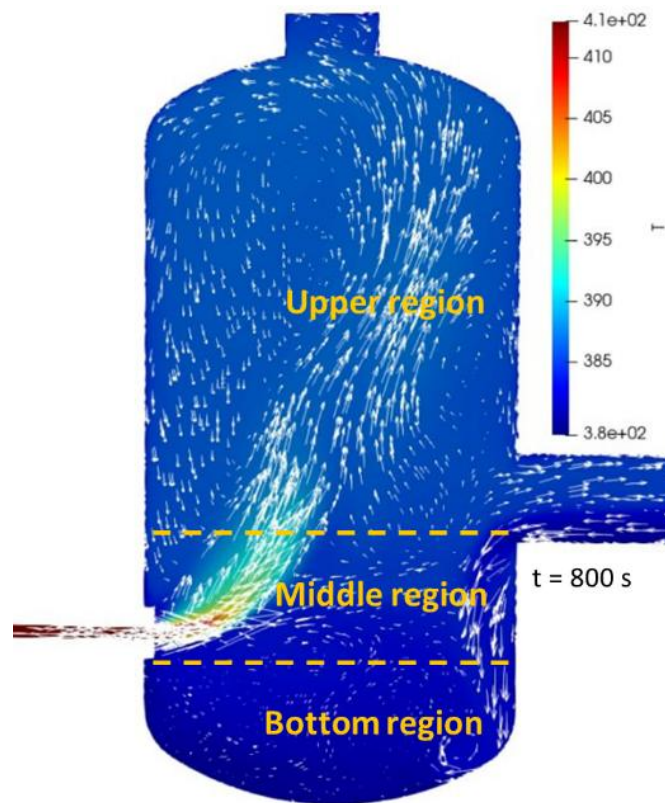


Fig. 4. Three regions on the Vessel 1.

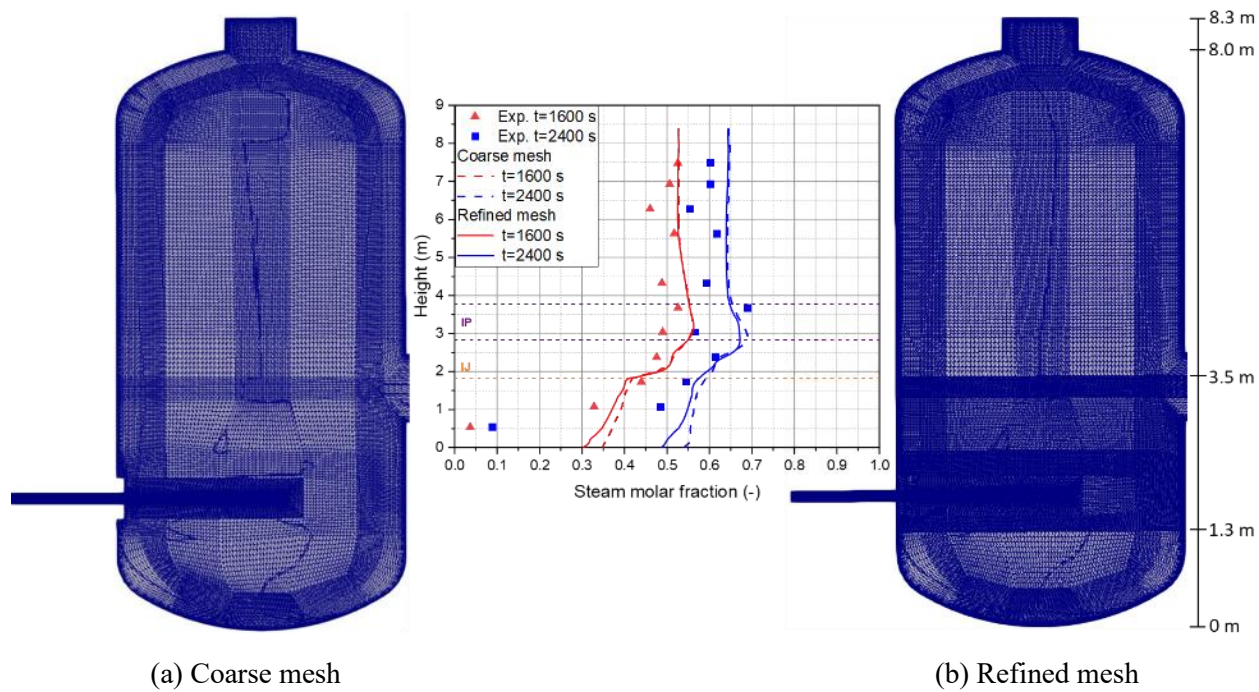


Fig. 5. Comparison with steam molar fraction between coarse and refined meshes.

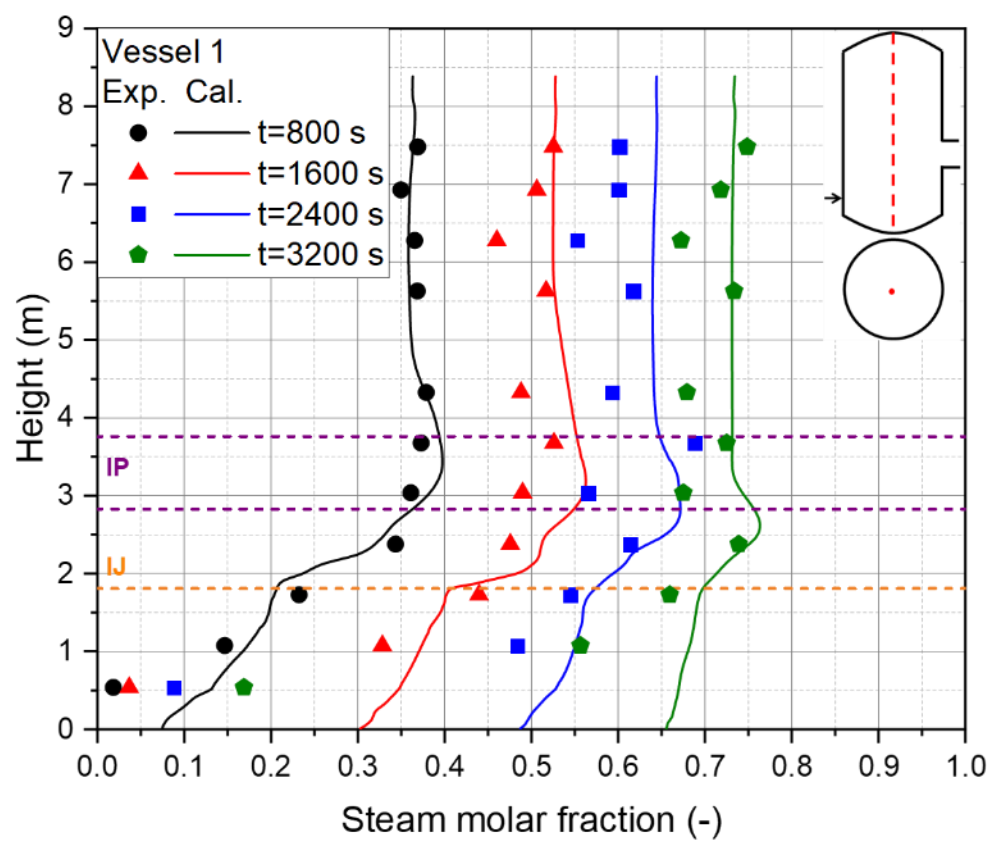


Fig. 6. Steam molar fraction according to height of Vessel 1.

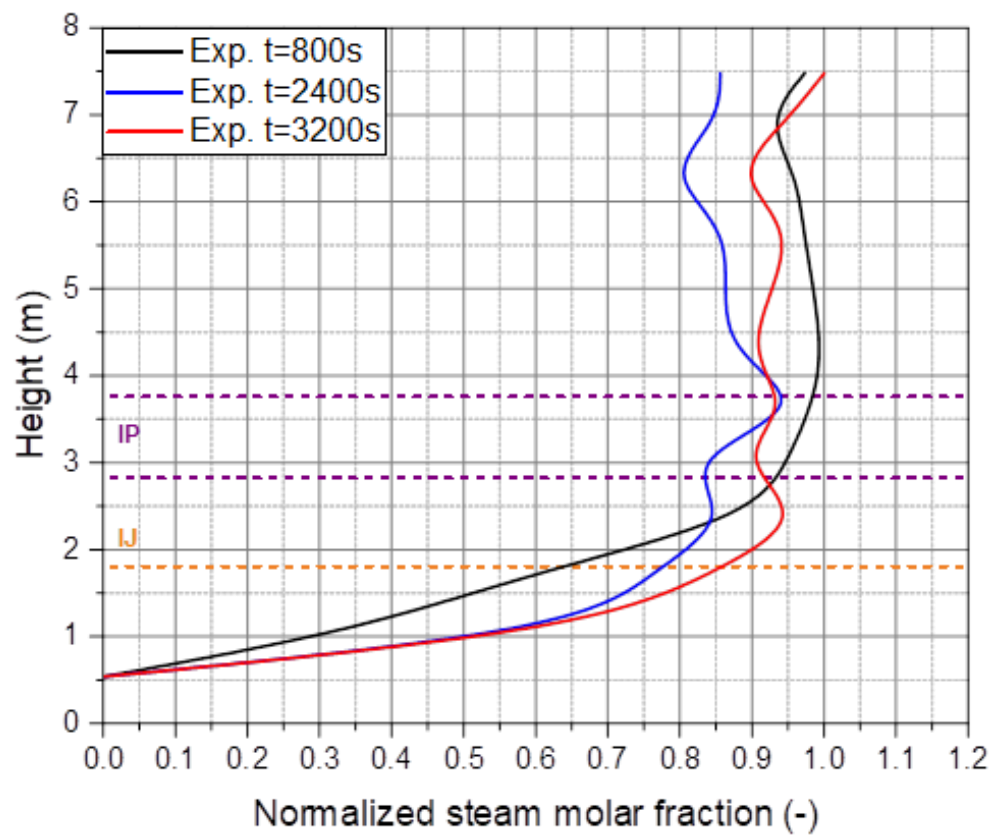


Fig. 7. Oscillating behavior of steam molar fraction over the height.

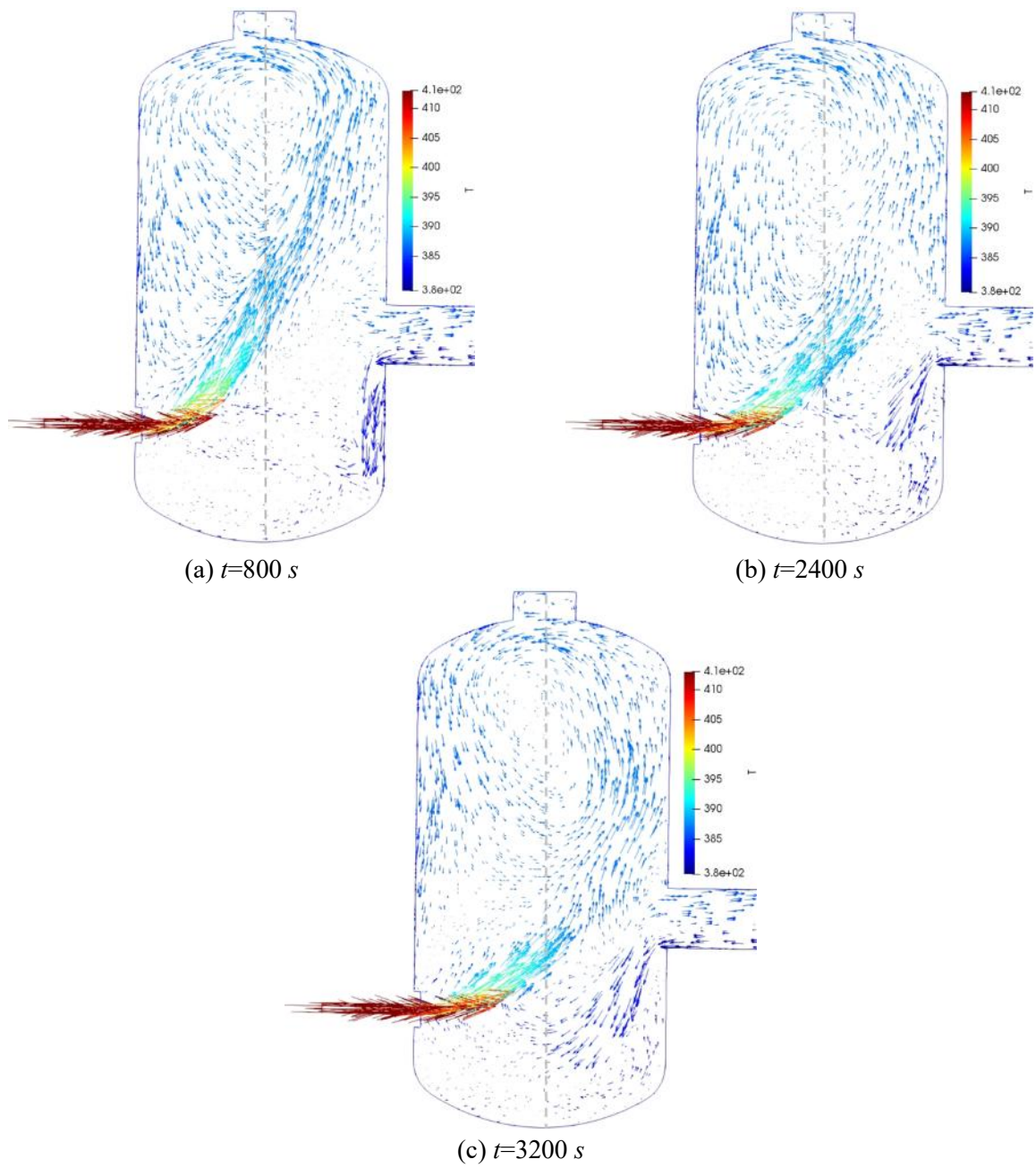


Fig. 8. Velocity vector for each time step in Vessel 1.

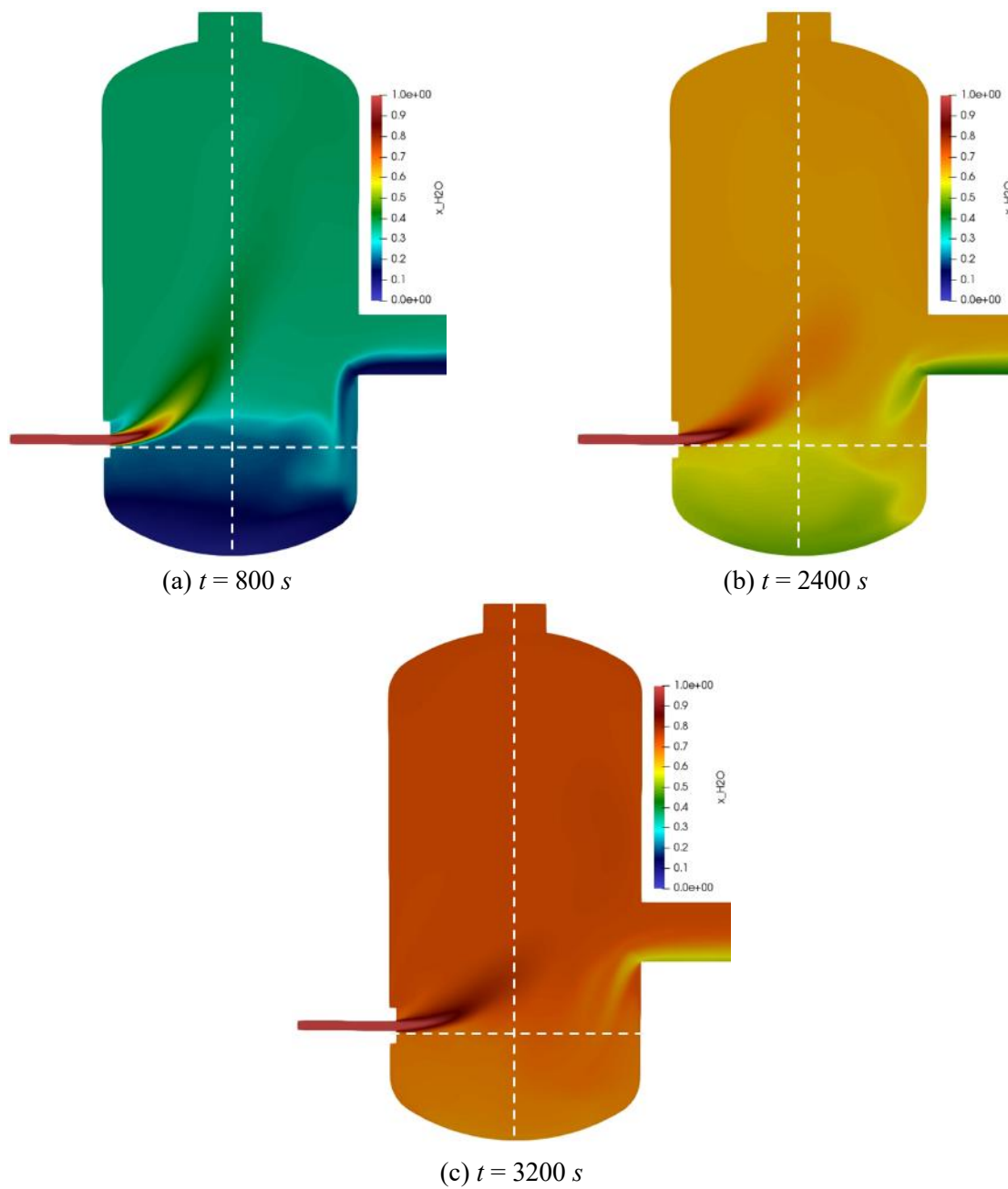
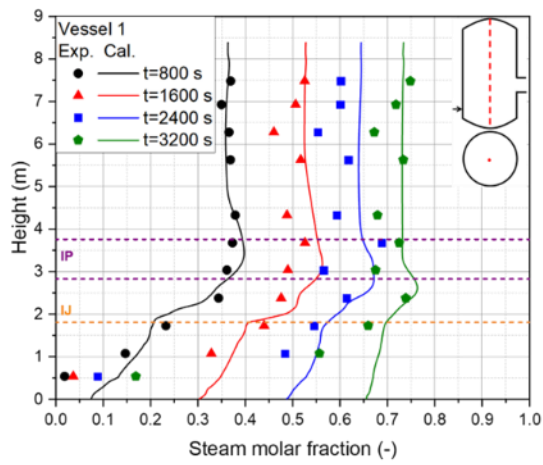
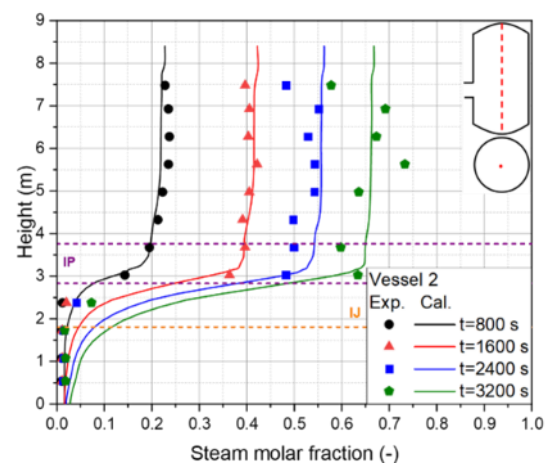


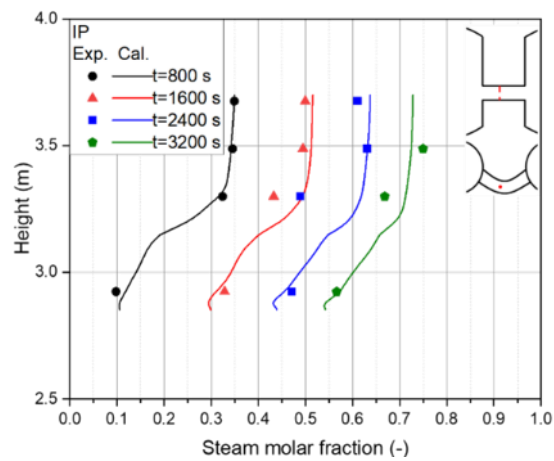
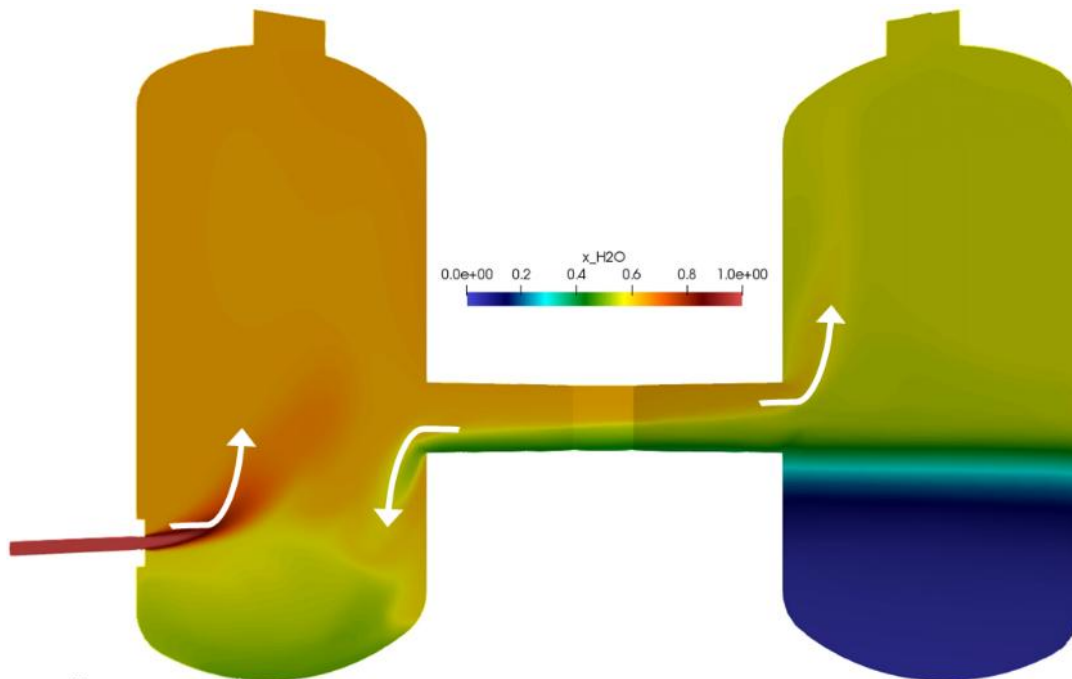
Fig. 9. Steam molar fraction fields for each time step (Vessel 1).



(a) Vessel 1



(b) Vessel 2



(c) IP

Fig. 10. Comparison steam molar fraction with Vessel 1, Vessel 2, and IP at 2400 s.

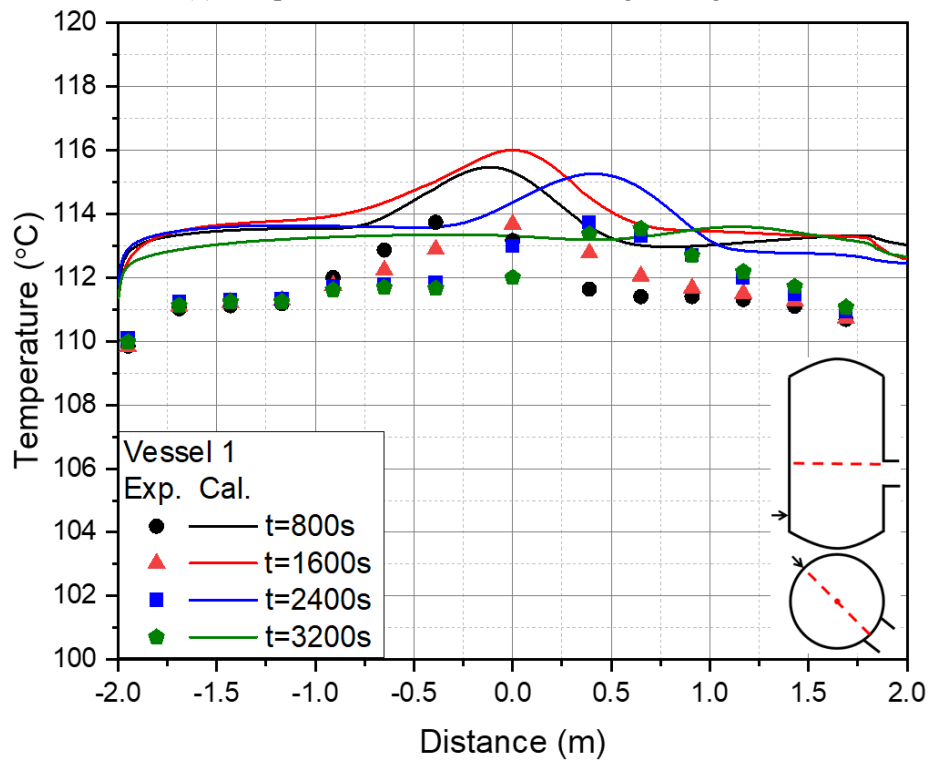
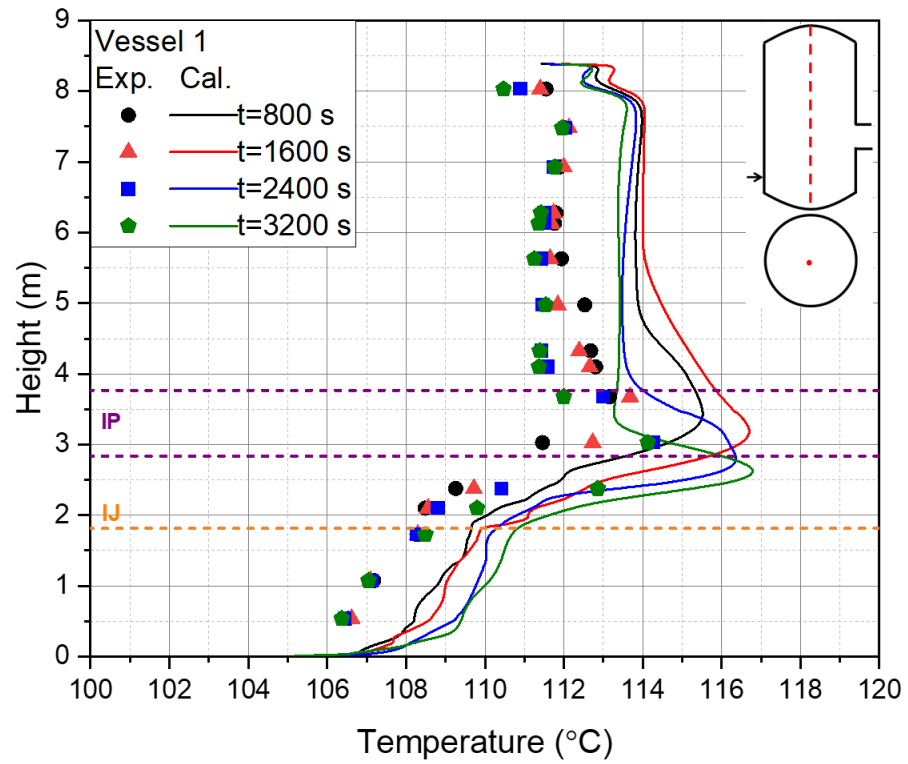
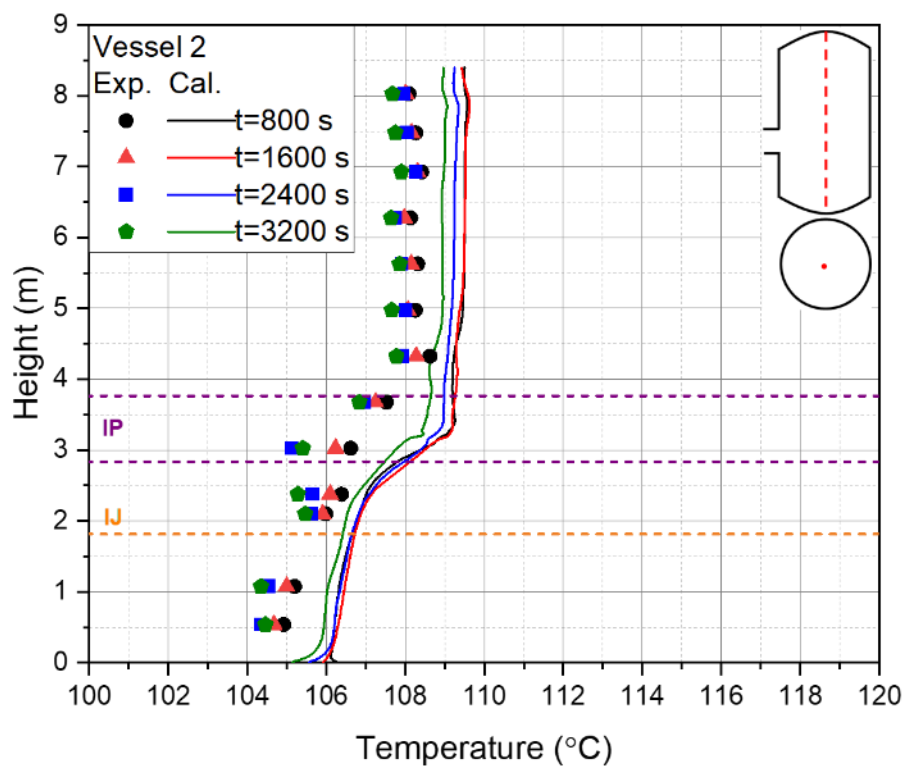
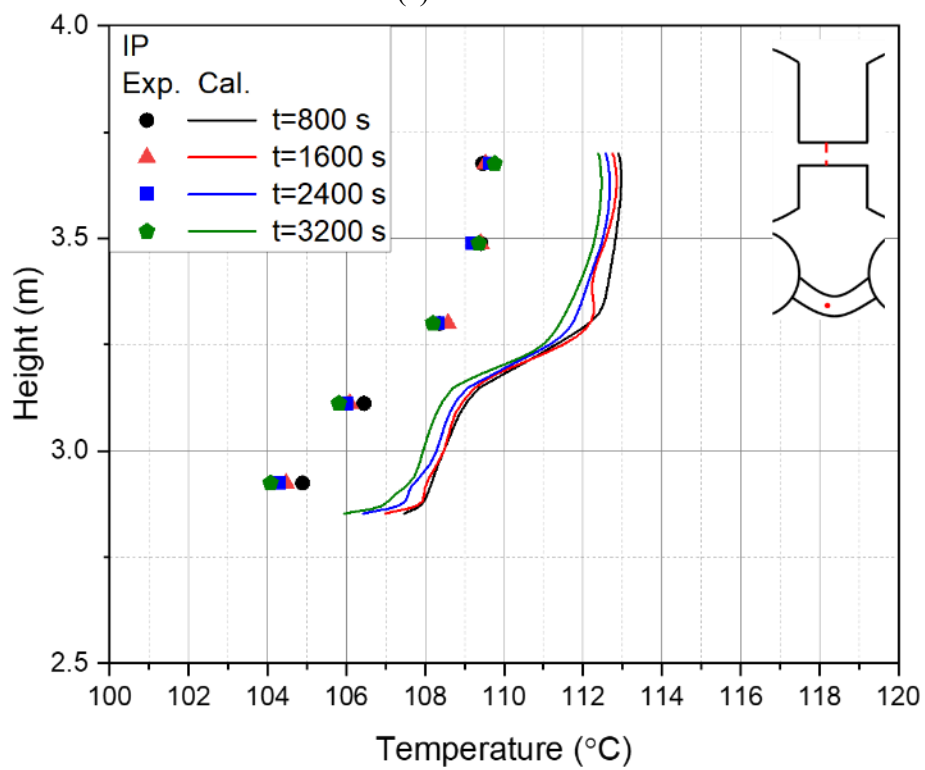


Fig. 11. Temperature distributions in Vessel 1.

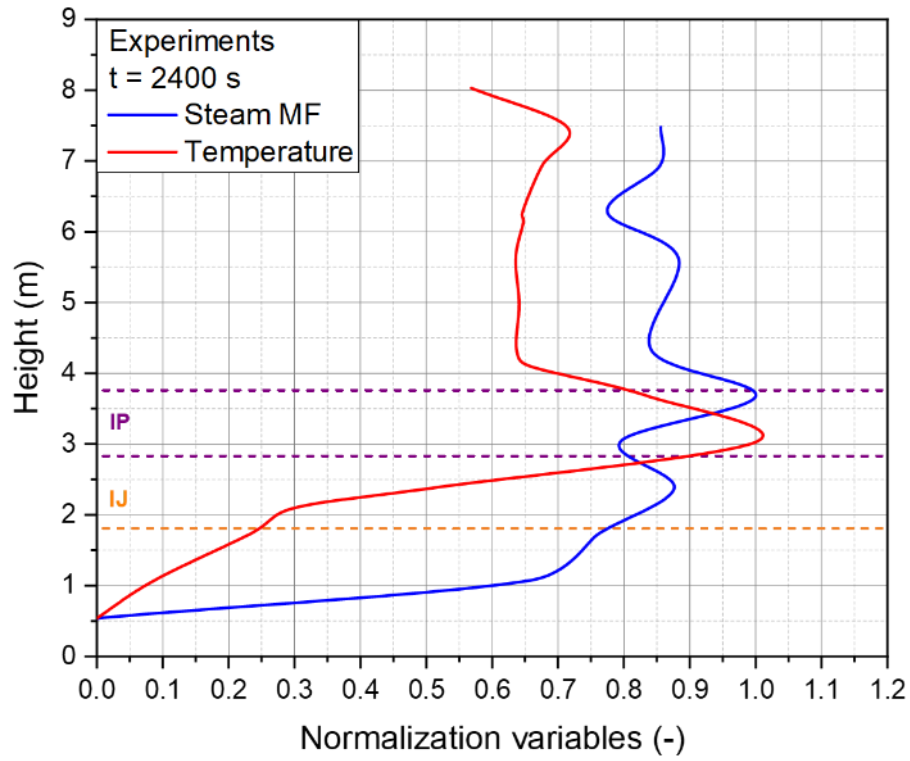


(a) Vessel 2

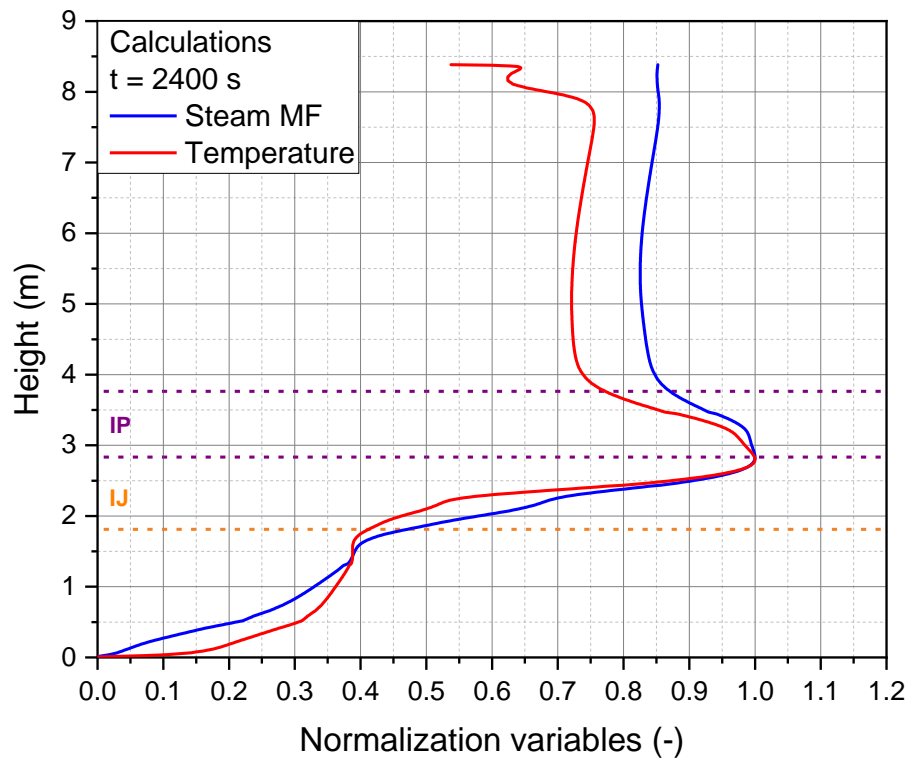


(b) IP

Fig. 12. Temperature distributions in Vessel 2 and IP.



(a) Experiments



(b) Calculation

Fig. 13. Comparison of distribution between steam molar fraction and temperature and over the height.

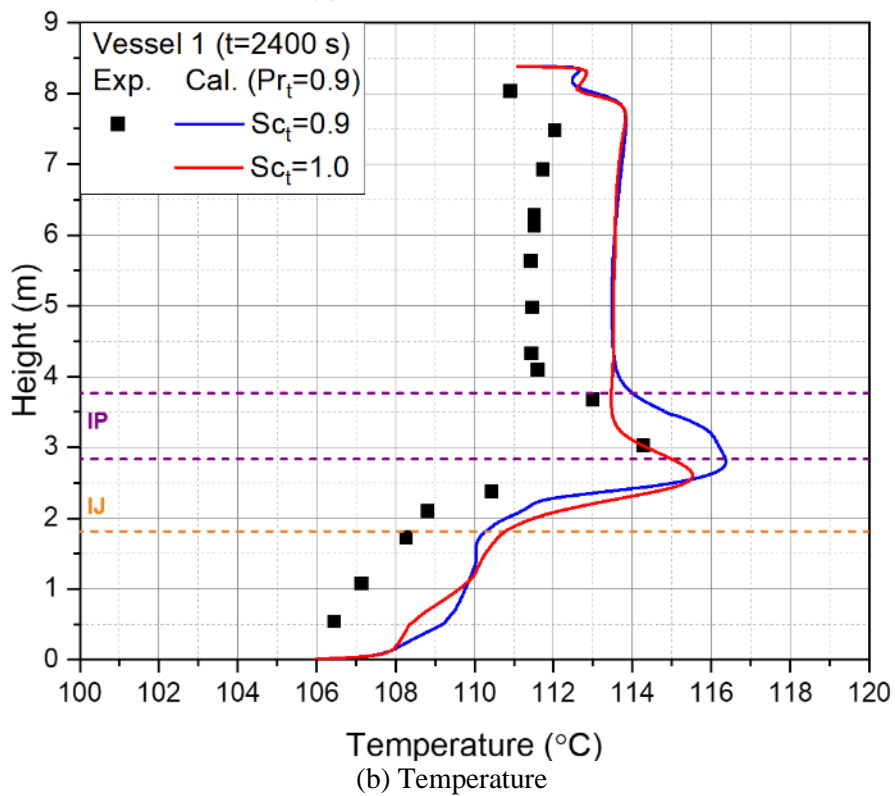
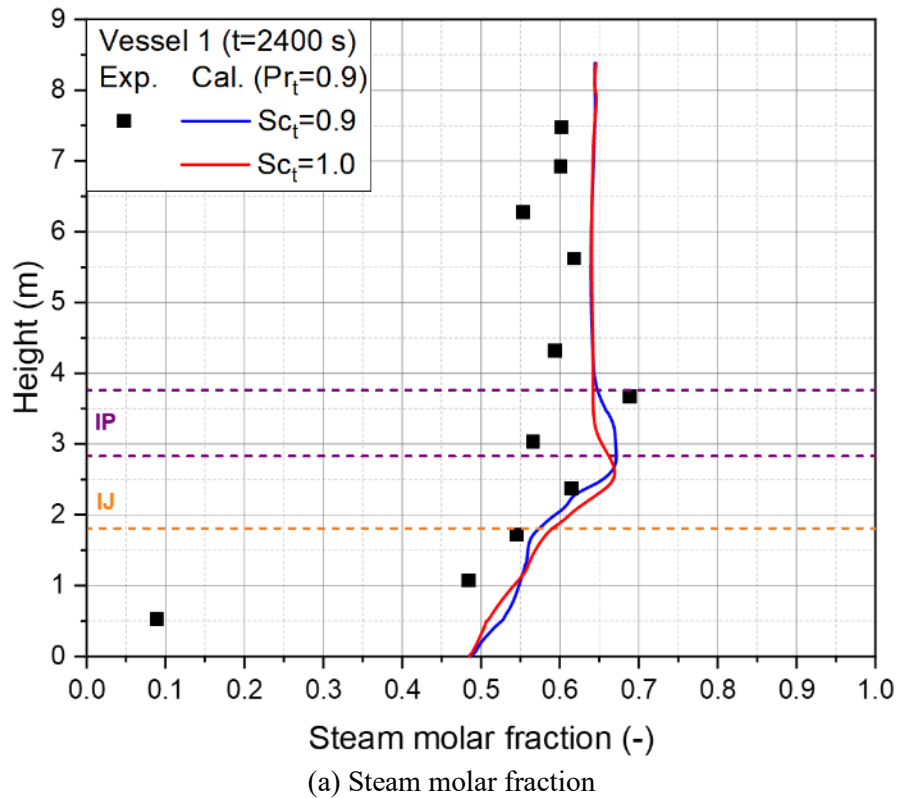


Fig. 14. Comparison of steam molar fraction and temperature over the $Sc_t = 0.9$ and 1.0 .